Spectroscopy and metastability of the HSS- anion

Besma Edhay, Souad Lahmar, Zohra Ben Lakhdar, Majdi Hochlaf

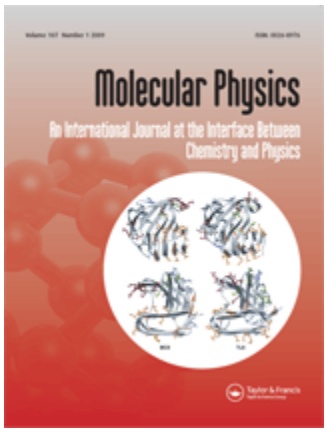

Spectroscopy and metastability of the HSS- anion

Journal:	*Molecular Physics*
Manuscript ID:	TMPH-2006-0048.R2
Manuscript Type:	Full Paper
Date Submitted by the Author:	21-Dec-2006
Complete List of Authors:	Edhay, Besma; University of Tunis, LSAMA LAHMAR, Souad; University of Tunis, LSAMA Ben Lakhdar, Zohra; Unversity of Tunis, LSAMA Hochlaf, Majdi; University of Marne La Vallee, Laboratoire de Chimie Theorique
Keywords:	Ab initio calculations, HSS anion, spectroscopy, ion molecule reaction

Spectroscopy and metastability of the HSS^- anion [#]

B. Edhay, S. Lahmar [a)] and Z. Ben Lakhdar

Laboratoire de Spectroscopie Atomique,

Moléculaire et Applications-LSAMA

Université de Tunis

Tunis, Tunisia

M. Hochlaf [b)]

Theoretical Chemistry Group

University of Marne-La-Vallée

Champs Sur Marne, F-77454,

Marne-La-Vallée, cedex 2, France

[#] Dedicated to Prof. Pavel Rosmus for his retirement.

---

a) E-mail: souad.lahmar@fsb.rnu.tn

b) Author to whom correspondence should be addressed. E-mail: hochlaf@univ-mlv.fr

Abstract

Accurate *ab initio* calculations on the potential energy surfaces (PESs) of the lowest electronic states of the neutral HSS and those of the electronic states of the HSS^- negative ion correlating to the bound asymptotes of this molecular system, reveal that the ground state of HSS^- (i.e. $\widetilde{X}\,^1A'$) and the long range parts of the anionic PESs are stable against the autodetachment processes. In light of these calculations, the $[HS + S]^-$ and $[S_2 + H]^-$ reactive systems are examinated and found forming the HSS^- ($\widetilde{X}\,^1A'$) ions either directly or after spin-orbit and / or vibronic and / or Renner-Teller couplings, in competition with fast electron loss processes. The three-dimensional PES of the unique bound electronic state of HSS^- (i.e. $\widetilde{X}\,^1A'$) is generated using the coupled cluster approach and a large basis set. A set of spectroscopic parameters for HSS^-/DSS^- ($\widetilde{X}\,^1A'$) and their vibrational spectra up to 3700 cm^{-1} are deduced from our 3D PES.

I. Introduction

Little is known about the thiosulfeno negative ion (HSS^-) in despite that its corresponding neutral molecule is widely studied [1]. These species as well as their positively charged ions are believed to play an important role in combustion and astrophysical chemistry and biochemistry [2-4]. The available experimental data for HSS^- are mostly due to the earlier photoelectron spectroscopic study of Moran and Ellison, who have determined the electron affinity (EA) of HSS to be 1.907 ± 0.023 eV [5]. Such large EA is expected for sulfur containing species [6]. These authors have also found that attaching an extra electron to the HSS ground state results mainly in a lengthening of the SS bond.

By stretching the SH internal coordinate, the HSS^- negative ion possesses three bound asymptotes {i.e. $S_2^-(X^2\Pi_g) + H(^2S)$; $S_2(X^3\Sigma_g^-) + H^-(^1S)$; $S_2(a^1\Delta_g) + H^-(^1S)$;}, which are located below the $S_2(X^3\Sigma_g^-) + H(^2S)$ dissociation limit. The Wigner-Witmer correlation rules applied to the $HSS^- \rightarrow [S_2 + H]^-$ molecular system show that the HSS^- ($1^3\Pi$, $1^1\Pi$, $1^3\Sigma^-$ and $1^1\Delta$) and their corresponding bent compounds should correlate to these three bound asymptotes. However, the lowest HSS^- ($1^1\Sigma^+$) state correlates adiabatically to the unbound $S_2(b^1\Sigma_g^+) + H^-(^1S)$ limit, which is located at 0.22 eV above $S_2(X^3\Sigma_g^-) + H(^2S)$. Along the SS coordinate, the $SH^-(X^1\Sigma^+) + S(^3P)$ and the $SH(X^2\Pi) + S^-(^2P)$ bound dissociation limits are located below the $SH(X^2\Pi) + S(^3P)$ neutral limit at 2.31 eV and 2.08 eV, respectively. In addition to the triatomic states given above, the $1^1\Sigma^-$, $1^3\Sigma^+$ and $1^3\Delta$ states are also correlating to these two asymptotes at large SS separations (far from the molecular region). This high density of electronic states should favor their mutual couplings, resulting in mixing of their electronic wavefunctions.

In the present work, the metastability of the HSS^- electronic states with respect to the autodetachment leading to $HSS + e^-$, is discussed in light of their potential energy surfaces, their electronic configurations and those of the neutral HSS molecule. It is worth noting that several conditions should be fulfilled by an anionic electronic state to exist: (i) it should possess positive electron affinity with respect to its parent neutral state; (ii) it should exhibit slow depletion by spin-forbidden autodetachment for at least one fine structure component and by radiative depletion; and (iii) its wavefunction should undergo weak interaction with the electron continuum wave. Here, large basis sets and multiconfigurational methods are used. Such large computations are needed for a good description of the anionic wavefunctions. However, our approach is not valid to describe accurately the negative ion resonances [7-9] (i.e. the PES parts located above the autodetachment thresholds), so that, only the bound parts of these PESs will be presented and discussed in next sections. In the last

part of the manuscript, the three-dimensional PES of the HSS^- ground state is generated and its bound vibrational term values are calculated variationally.

II. Computational methods

The electronic calculations were performed using the complete active space self-consistent field (CASSCF) approach [10] followed by the internally contracted multi-reference configuration interaction including the Davidson correction (MRCI+Q) method [11,12] and the Coupled Cluster technique including the quasi-perturbative treatment of the connected triple substitutions (CCSD(T)) [13], which are implemented in the MOLPRO program suite [14]. The sulfur atoms were described using a large basis set of *spdfgh* aug-cc-pV5Z quality [15] and the hydrogen was described with the *spdfg* aug-cc-pV5Z Dunning's basis set [16], resulting in 342 contracted Gaussian functions. In these calculations, the CASSCF active space included all configurations (CSFs configuration state functions) obtained after excitations of all valence electrons in valence orbitals. In the C_{2v} point group (collinear SS or SH elongations), this results in 172 (162), 130 (160), 130 (160) and 108 (148) CSFs for the singlets (for the tripltes) in the A_1, B_1, B_2 and A_2 symmetries, respectively. Moreover, all electronic states with the same spin multiplicity have been averaged together using the CASSCF averaging procedure implemented in MOLPRO, where 3 (4) A_1, 2 (2) B_1, 2 (2) B_2 and 3 (4) A_2 components were considered for the singlets (for the triplets). For MRCI calculations, all configurations in the CI expansion of the CASSCF wavefunctions were taken as a reference. For HSS^-, this results in more than 130 x 10^6 CSFs to be treated in the C_{2v} point group. All valence electrons were correlated. The present calculations were performed in both the C_{2v} (for the collinear PES cuts) and the C_s (for bent structures) point groups.

The three-dimensional PES of the HSS^- ($X\ ^1A'$) electronic ground state has been mapped in the internal coordinates of this anion corresponding to the SH (R_{SH}), SS (R_{SS}) stretchings and to the bending angle (θ), at the *spdfg*(*h*) aug-cc-pV5Z/CCSD(T) level of theory. The calculations were carried out for 45 different geometries, so that the near equilibrium and the bound parts of this PES are covered (up to ~ 10000 cm^{-1} above the minimum). The calculated energies were fitted to a polynomial expansion (*cf. infra*). This analytical form was used later to calculate the quartic force field in internal coordinates, which has been transformed by the *l*-tensor algebra to quartic force field in dimensionless normal coordinates [17,18]. These data allow us to evaluate a set of spectroscopic properties using second order perturbation theory. The PES expansion was also used in variational calculations using the approach of Carter and Handy [19]. The vibrational energies up to 3700 cm^{-1} are deduced for HSS^- $\tilde{X}$ and DSS^- $\tilde{X}$. The accuracy of the vibrational term values should be better than 10-20 cm^{-1} with comparison to similar works for other triatomic negative ions [21-22].

III. Electronic States of HSS^-

The anionic states in interest here are obtained by attaching an extra electron to the 3a" or to the 14a' or to the 15a' orbitals and present either the HSS ($\widetilde{X}\,^2$A") or the HSS (1^2A') as parent states. For further details readers are referred to Table I. Figure I depicts the MRCI+Q one-dimensional cuts of the three-dimensional potential energy surfaces of the electronic states of HSS^- for bent structures. Only the bound parts are presented. These curves are given in energy with respect to the HSS ($\widetilde{X}\,^2$A") minimum. They are obtained by varying the SS (R_{SS}, in A) and the SH (R_{SH}, in B) internal coordinates, where the bending angle is kept fixed at 102° and the R_{SH} = 2.5 bohr or the R_{SS} = 3.9 bohr (1 bohr = 1 a_0 = 0.529 Å) corresponding to their equilibrium values in HSS^- ($\widetilde{X}\,^1$A') (see below). The dissociation limits are positioned using our dissociation energies (D_e) for HSS ($\widetilde{X}\,^2$A"), the experimentally determined electron affinities (EA) of S (~ 2.08 eV), of SH (~ 2.31 eV), of S_2 (~ 1.670 eV) and of H (0.754 eV), and the electronic transition energies of S_2 [6]. Our D_e's are computed at the aug-cc-pV5Z/MRCI+Q level of theory including the Basis Set Superposition Error (BSSE). It is calculated 2.76 eV (2.86 eV) along the SS (SH) coordinate.

At large internuclear separations, Figure I shows a high density of electronic states for the HSS^- anion favoring their mutual couplings by vibronic (between the electronic states having the same spin multiplicity) and spin-orbit (between the singlets and the triplets), and complicating the computations for this molecular system. Some anionic states are lying so close in energy that one can not clearly distinguish them there. This is the case, for instance, for the 2^3A', the 2^1A", 2^3A" states (cf. Figure I A).

Figure II presents the MRCI+Q one-dimensional PES cuts evolution of the HSS ($\widetilde{X}\,^2$A", 1^2A' and 1^4A") states and the bound parts of those of HSS^- along the bending coordinate. These curves are obtained by varying the bending angle (θ), where the stretches are set to R_{SH} = 2.5 and R_{SS} = 3.9, in bohr. This figure shows that the neutral doublet states correlate to the same $\widetilde{X}\,^2\Pi$ state at linearity forming a bent/bent Renner-Teller system. The neutral quartet correlates to the lowest $^4\Sigma^-$ state for θ = 180°. It is worth noting also that the HSS^- ground state is a singlet of A' symmetry species, correlating to the lowest $^1\Sigma^+$ state at linearity. This ground state possesses a bent equilibrium geometry with a bending angle close to the equilibrium bending angle of HSS (X^2A"). Moreover, the two lowest triplets form a linear/bent Renner-Teller pair, leading to the $1^3\Pi$ state at linearity. Finally, the two upper singlets are coupled by Renner-Tenner effect via the $1^1\Pi$ state, which is however, found to be located above the autodetachment threshold for these internuclear distances.

Figure III displays the aug-cc-pV5Z/MRCI+Q one-dimensional cuts of the 3D PES of the electronic states of HSS^- and those of HSS ($\widetilde{X}\,^2\Pi$ & $^4\Sigma^-$) for collinear configurations, along the SS stretching (R_{SS}, in Figure III A) and along the SH distance (R_{SH}, in Figure III B). Among the anionic electronic states depicted there, only the $1^1\Sigma^+$ to which the HSS^- ($\widetilde{X}\,^1A'$) state correlates adiabatically, possesses a deep potential well along both the SS and SH internal coordinates. The other states are repulsive in nature at least when the SS distance is lengthened. In despite that several electronic states are located below the lowest neutral states for linear configurations, they will exhibit fast electron loss when the molecule is bent (cf. Figure II), exception should be made for the lowest singlet leading to HSS^- ($\widetilde{X}\,^1A'$) minimum.

Close examination of Figures I-III and Table I reveals that our anionic electronic states are bound at large internuclear distances since they are located below their respective parent states. The situation is, however, quite different in the molecular region and only the anionic electronic ground state {i.e. HSS^- ($\widetilde{X}\,^1A'$)} fully fulfills the metastability conditions given above. Indeed, this electronic state is located well below its parent state {i.e. HSS ($\widetilde{X}\,^2A''$)} for both linear and bent configurations and it is located in energy far from the upper electronic states so that it is free from any interaction. In contrary, the anionic exited states are crossing the HSS ($\widetilde{X}\,^2A''$) PES close to the molecular region where fast electron loss is expected to occur either directly (for those presenting the HSS ($\widetilde{X}\,^2A''$) as parent state), or indirectly after spin-orbit and / or vibronic couplings (for those accessed by bending an extra electron to the HSS($1^2A'$)). This is confirming the Photo Electron Spectroscopy results of Moran and Ellison, which found a unique stable electronic state for HSS^- [5]. Finally and by inspection of our data depicted in Figures I-III, the EA value of HSS is computed ~1.75 eV at the *spdfg(h)* aug-cc-pV5Z/MRCI+Q level of theory, which is 0.16 eV lower than the experimental value (1.907 ± 0.023 eV [5]). Such differences between the experimental and the theoretical EA determinations are commonly admitted for similar calculations of this quantity. See Refs. [7-9, 23] for detailed discussions.

In light of the present theoretical results, we would like to discuss also the reactivity of HS/HS^- against S^-/S and its of S_2/S_2^- + H^-/H. When the reactants are taken in their electronic ground states, these reactions follow the PES of HSS^- ($\widetilde{X}\,^1A'$) for bent structures and lead directly to the formation of this negative ion. However, when the reactants are electronically excited and /or for collinear collisions, the reactions may follow first the PES of the HSS^- excited states, forming the electronically excited HSS^- ions transiently, which may be converted later into the HSS^- ($\widetilde{X}\,^1A'$) ions after spin-orbit and / or vibronic and / or Renner-Teller (for the doubly degenerate electronic states) interactions in competition with the autodetachment processes.

IV. Spectroscopy of the ground states of HSS^- and of DSS^-

A polynomial function of the form

$$V(Q_1, Q_2, Q_3) = \Sigma_{ijk} C_{ijk} (Q_1)^i (Q_2)^j (Q_3)^k$$

where $Q_i = (R_i - R_i^{ref})/R_i$, for i = 1,2

and $Q_3 = \theta - \theta^{ref}$

The index 'ref' refers to the reference geometry used during the fit, which is taken the equilibrium geometry of HSS^- ($\widetilde{X}\,^1A'$) here. R_1, R_2 correspond to the SS and the SH stretching coordinates respectively and θ is the bending coordinate. The i, j, k exponents were restricted to i+j+k ≤4. 35 C_{ijk} coefficients were optimized using a least square procedure. These terms are given in Table II. The root mean square of the fit was less than 8 cm^{-1}.

Table III lists the quartic force fields of HSS^- ($\widetilde{X}\,^1A'$) and of DSS^- ($\widetilde{X}\,^1A'$) in dimensionless normal coordinates. It turns out from these values that some couplings do exist between the SH stretch and the bending modes, since both the third and fourth order force field terms relative to these modes (for instance ϕ_{221} = 510.2 cm^{-1} and ϕ_{2211} = -527.1 cm^{-1}) have large values. However, only weak coupling is expected between the two stretching modes.

Table IV gives the equilibrium geometry of HSS^-($\widetilde{X}\,^1A'$) deduced from our 3D CCSD(T) PES. The R_{eSS} distance is computed 2.091 Å and the R_{eSH} is calculated 1.343 Å. The accuracy of our calculated equilibrium distances should be better than 0.01 Å.The angles of HSS (101.74° [24,25]) and of HSS^- (101.8°) are close to each other. We have also done a systematic geometry optimization of the equilibrium geometry of this electronic state at the cc-pV6Z/CCSD(T) level of theory. The results are close to the one deduced from our 3D PES and those obtained by Owens et al [26] (cf. Table IV). Accordingly, the formation of HSS^- ($\widetilde{X}\,^1A'$) by attaching an electron to HSS ($\widetilde{X}\,^2A''$) is accompanied by a lengthening of the SS bond (ΔR_{SS} ~ 0.13 Å) and a slight shortening of the SH distance (ΔR_{SH} ~ 0.01 Å) [24,25]. The changes are more significant for the SS distance in good accord with Moran and Ellison's Franck-Condon analysis of their PhotoElectron spectrum of HSS^-. [5].

In Table IV are also listed the spectroscopic parameters of HSS^- ($\widetilde{X}\,^1A'$) and of DSS^- ($\widetilde{X}\,^1A'$) obtained using second order perturbation theory. They include the rotational constants (A_e, B_e, C_e), the harmonic wavenumbers (ω_i) the vibration-rotation terms (α_i) and the anharmonicity terms (x_{ij}). This table shows that HSS^- is an asymmetric top molecule with B_e ~ C_e. Our harmonic wavenumbers are computed ω_1 = 2594.4 (SH stretching), ω_2 = 829.8 (bending) and ω_1 = 484.6 (SS stretching), in cm-1,

which are in good accord with the values of Ref. [26]. The variationally computed SH anharmonic wavenumber (ν_1) is calculated 2453.6 cm^{-1}. The SS stretch and the bending are calculated ν_3 = 478.8 cm^{-1} and ν_2 = 808.8 cm^{-1}, respectively, which are distinctly smaller than their corresponding values for HSS $\widetilde{X}$ (i.e. $\nu_2 = 904 \pm 8$ cm^{-1} and $\nu_3 = 595 \pm 4$ cm^{-1} [27]), where as the SH stretchs for the anion and the neutral molecule (ν_1 = 2463 cm^{-1} [28]) are close to each other.

Table V gives the vibrational theoretical energies of HSS^- ($\widetilde{X}\,^1A'$) and its isotopomer. The calculations are carried out for J=0. Here, anharmonic resonances can be found between their vibrational term values even for the ones located as low as 2000 cm^{-1} (they are marked by an asterisk in Table V). For example, the level of HSS^- $\widetilde{X}$ located at 2538.5 cm^{-1} is a mixture of (0,2,2), (0,1,3), (0,3,1) and (0,3,3) with the highest contribution from (0,2,2). Such resonances mix the vibrational wavefunctions of these levels making their assignment by quantum numbers quite difficult. For these reasons the attributions given in Table V are only tentative for energies >2000 cm^{-1} with respect to the zero point vibrational energy (ZPE) except the levels involving the SH stretching. For DSS^-, the isotopic shifts are calculated variationally to be ~662 cm^{-1} for ν_1, which is associated with the strongest reduction due to the H/D substitution; and ~ 220 cm^{-1} for ν_2. However, no significant change is found for ν_3 since it corresponds mainly to the SS elongation. These isotopic shift values are consistent with those observed for the neutral DSS and for the DSS^+ cation [6]. Since the Franck-Condon Factors (FCFs) for the H/DSS^- ($\widetilde{X}\,^1A'$) + hν → H/DSS ($\widetilde{X}\,^2A''$) + e^- process, correspond mostly to the excitation of the SS stretching mode (ν_3) and the isotopic shift for this mode is distinctly smaller than the PhotoElectron Spectroscopy experimental resolution (of ~ 160 cm^{-1} [5]), the corresponding spectra for HSS^- and for DSS^- should have similar shapes with relatively few differences, which is consistent with the data given in Ref. [5].

V. Conclusion

Accurate *ab initio* computations are performed on the HSS^- electronic states correlating to the bound asymptotes of this molecular system and those of their respective neutral parent states. In light of these calculations, the stability of the electronic states of this anion has been treated, confirming the experimental findings that HSS^- does possess a unique stable electronic state of $^1A'$ symmetry. This electronic state is found to support several rovibrational levels located below the autodetachment threshold corresponding to the vibrational ground state of HSS ($\widetilde{X}\,^2A''$). The present theoretical predictions are also used for discussing the reactions leading to the formation of HSS^- when S/S^- (H/H^-) and SH^-/SH (S_2^-/S_2) are colliding together, which are viewed to follow the PES of HSS^- $\widetilde{X}$ and the long range parts of the PESs of the HSS^- electronic excited states. These reactions are occurring in

competition with the autodetachment processes. Finally, a set of accurate spectroscopic data are computed for HSS^- $\widetilde{X}$ that should be helpful for identifying this triatomic negative ion in the interstellar media and in laboratory.

Acknowledgments

M. H. would like to thank a visiting fellowship from the University of Tunis.

References

1. P. A. Denis. Chem. Phys. Lett. **422**, 434 (2006) and references therein.
2. R. J. Huxtable. Biochemistry of sulphur, Plenum Press, New York (1986).
3. P. A. Denis. Chem. Phys. Lett. **402**, 289 (2005).
4. P. A. Denis and O. N. Ventura. Chem. Phys. Lett. **344**, 221 (2001).
5. S. Moran and G. B. Ellison. J. Chem. Phys. **92**, 1794 (1988).
6. http://webbook.nist.gov.
7. M. Hochlaf, G. Chambaud, P. Rosmus, T. Andersen and H. J. Werner. J. Chem. Phys. **110**, 11835 (1999) and references therein.
8. S. Ben Yaghlane, S. Lahmar, Z. Ben Lakhdar and M. Hochlaf. J. Phys. B **38**, 3395 (2005).
9. A. Dreuw, T. Sommerfeld and L. S. Cederbaum. J. Chem. Phys. **116**, 6039 (2002) and references therein.
10. P. J. Knowles and H.-J. Werner. Chem. Phys. Lett. **115**, 259 (1985).
11. H.-J. Werner and P. J. Knowles. J. Chem. Phys. **89**, 5803 (1988).
12. P. J. Knowles and H.-J. Werner. Chem. Phys. Lett. **145**, 514 (1988).
13. C. Hampel, K.A. Peterson and H.-J Werner. Chem. Phys. Lett. **190**, 1 (1992).
14. MOLPRO is a package of *ab initio* programs written by H. J. Werner and P. J. Knowles. Further details at www.tc.bham.ac.uk/molpro.
15. D. E. Woon and T. H. Dunning. Jr. J. Chem. Phys. **98**, 1358 (1993).
16. T. H. Dunning. J. Chem. Phys. **90**, 1007 (1989).
17. J. Senekowitsch, thesis of the University of Frankfurt, Germany (1988).
18. I. M. Mills, in '*Molecular Spectroscopy : Modern Research*', Ed. K. N. Rao and C. W. Mathews, Academic Press, 1972.
19. S. Carter, N. C. Handy. Comput. Phys. Rev. **5**, 117 (1987).
20. C. Léonard, D. Panten, N.M. Lakin, G. Chambaud and P. Rosmus. Chem. Phys. Lett. **335**, 97 (2001).
21. C. Léonard, D. Panten, P. Rosmus, M. Wyss and J.P. Maier. Chem. Phys. **264**, 267 (2001).
22. C. Léonard, D. Panten, P. Rosmus, M. Wyss and J.P. Maier. Collect. Czech. Chem. Commun. **66**, 983 (2001).
23. B. Edhay, S. Lahmar, Z. Ben Lakhdar and M. Hochlaf. Progress in Theoretical Chemistry and Physics series, Ed. S. Wilson, (2007), in press.
24. S. Yamamoto and S. Saito. Can. J. Phys. **72**, 974 (1994).
25. Y. Tanimoto, T. Klaus. H. S. P. Muller and G. Winnewisser. J. Mol. Spectrosc. **199**, 73 (2000).
26. Z. T. Owens. J. D. Larkin and H. F. Schaefer III. J. Chem. Phys. **125**, 164322 (2006).
27. A. B. Sannigrahi, S. D. Peyerimhoff and R. J. Buenker. Chem. Phys. Lett. **46**, 415 (1977).
28. C. Lee, W. Yang and R. G. Parr. Phys. Rev. B, 785 (1985).
29. M. Kraus and S. Rosak. J. Phys. Chem. **96**, 8325 (1992).

Table I: Dominant electron configurations of the electronic states of HSS^- and HSS investigated presently. These configurations are quoted for R_{SS}=3.9 bohr, R_{SH}=2.5 bohr and θ = 140°.

State	Electron configuration
HSS($\widetilde{X}\,^2$A")	…$(13a')^2(14a')^0(15a')^0(2a")^2(3a")^1$
HSS(1^2A')	…$(13a')^1(14a')^0(15a')^0(2a")^2(3a")^2$
HSS(1^4A")	…$(13a')^1(14a')^1(15a')^0(2a")^2(3a")^1$
HSS^-($\widetilde{X}\,^1$A')	…$(13a')^2(14a')^0(15a')^0(2a")^2(3a")^2$
HSS^-(2^1A')	…$(13a')^1(14a')^1(15a')^0(2a")^2(3a")^2$
HSS^-(1^1A")	…$(13a')^2(14a')^1(15a')^0(2a")^2(3a")^1$
HSS^-(2^1A")	…$(13a')^2(14a')^0(15a')^1(2a")^2(3a")^1$
HSS^-(1^3A')	…$(13a')^1(14a')^1(15a')^0(2a")^2(3a")^2$
HSS^-(2^3A')	…$(13a')^1(14a')^0(15a')^1(2a")^2(3a")^2$
HSS^-(1^3A")	…$(13a')^2(14a')^0(15a')^1(2a")^2(3a")^1$
HSS^-(2^3A")	…$(13a')^2(14a')^1(15a')^0(2a")^2(3a")^1$

Table II: C_{ijk} coefficients of the 3D PES expansion of HSS^- ($\tilde{X}\,^1A'$). See text.

C_{200}	1.1679279356	C_{110}	0.0814196421	C_{011}	-0.0440543365
C_{020}	0.8006828562	C_{101}	0.1323282354	C_{210}	-0.2403054745
C_{002}	0.0813695753	C_{300}	-1.5108646006	C_{201}	-0.2784954714
C_{120}	0.2954557506	C_{030}	-0.5414964790	C_{102}	-0.2160236364
C_{111}	0.0369662108	C_{021}	-0.0817846500	C_{400}	0.0049308279
C_{012}	-0.0113640627	C_{003}	0.0033473528	C_{130}	0.2993250306
C_{310}	0.0791335309	C_{220}	-0.4331797664	C_{211}	0.0523300287
C_{040}	-0.5020792556	C_{301}	-0.3118392838	C_{202}	0.0506992063
C_{121}	-0.0612625150	C_{031}	-0.0593922840	C_{103}	-0.0542080560
C_{112}	-0.0501480901	C_{022}	-0.0094558269	C_{013}	0.0571900248
C_{004}	-0.0176684380				

Table III: Quartic force fields of HSS^- ($\tilde{X}\,^1A'$) and DSS^- ($\tilde{X}\,^1A'$) in dimensionless normal coordinates. All values are in cm^{-1}. See text for more details.

Quartic force field	HSS^-	DSS^-
ω_1	2594.4	1863.9
ω_2	829.8	600.2
ω_3	484.6	484.4
ϕ_{333}	-149.7	-149.3
ϕ_{222}	6.83	4.21
ϕ_{111}	-1780.78	-1082.2
ϕ_{332}	-5.65	-6.68
ϕ_{322}	-69.4	-51.3
ϕ_{331}	7.2	9.79
ϕ_{221}	510.2	290.6
ϕ_{312}	-96.9	-72.3
ϕ_{311}	71.9	51.7
ϕ_{211}	-120.6	-77.0
ϕ_{3333}	40.9	40.9
ϕ_{2222}	297.6	131.3
ϕ_{1111}	1003.4	516.4
ϕ_{3332}	-0.76	-0.25
ϕ_{3222}	-62.6	-36.7
ϕ_{3322}	15.2	12.0
ϕ_{3331}	3.6	3.2
ϕ_{2221}	-71.3	-36.1
ϕ_{3321}	-8.84	-7.0
ϕ_{3221}	36.6	22.1
ϕ_{3311}	-19.1	-16.1
ϕ_{2211}	-527.1	-256.3
ϕ_{3211}	94.2	60.5
ϕ_{3111}	-38.8	-24.2
ϕ_{2111}	96.9	52.6

Table IV: Structural and spectroscopic parameters of $HSS^-(\tilde{X}\,^1A')$ and $DSS^-(\tilde{X}\,^1A')$ deduced from our three-dimensional potential energy surface using second order perturbation theory and including the equilibrium geometry (R_{eSS}, R_{eSH} and θ_e), rotational constants (A_e, B_e, C_e), harmonic (ω_i) wavenumbers, vibration-rotation terms (α_i) and anharmonicity terms (x_{ij}).

	$HSS^-(\tilde{X}\,^1A')$	$DSS^-(\tilde{X}\,^1A')$
R_{eSS}/Å	2.091 2.089 [a)] 2.121 [b)] 2.101 [c)]	
R_{eSH}/Å	1.343 1.346[a)] 1.332 [b)] 1.348 [c)]	
θ_e/degree	101.8 101.6[a)] 101.0 [b)] 101.4 [c)]	
A_e/MHz	302035.8	157332.7
B_e/MHz	7050.1	6877.6
C_e/MHz	6889.3	6589.6
ω_1/cm^{-1}	2594.4 2599 [c)]	1863.9
ω_2/cm^{-1}	829.8 822 [c)]	600.2
ω_3/cm^{-1}	484.6 478 [c)]	484.4
α_1^A /MHz	9598.7	3472.9
α_2^A /MHz	-6188.8	-2359.3
α_3^A /MHz	226.5	129.1
α_1^B /MHz	-27.1	-14.3
α_2^B /MHz	19.2	6.4
α_3^B /MHz	46.5	43.9
α_1^C /MHz	-21.4	-7.7

α_2^C /MHz	31.1	19.5
α_3^C /MHz	46.1	45.0
x_{11}/cm^{-1}	-68.1	-35.1
x_{22}/cm^{-1}	-5.75	-2.9
x_{33}/cm^{-1}	-2.26	-2.2
x_{12}/cm^{-1}	-13.7	-7.1
x_{13}/cm^{-1}	2.31	1.7
x_{23}/cm^{-1}	-4.85	-3.7

a) This work. Geometry optimized at the cc-pV6Z/CCSD(T) level of theory.

b) *Spd* cc-pVDZ/SCF calculations. Ref. [29]

c) Calculated at the aug-ccpVQZ/CCSD(T). Ref. [26].

Table V: Variationally computed vibrational term values of the electronic ground states of HSS^- and of DSS^-. The asterisk denotes anharmonic resonances (see text).

$HSS^-(\tilde{X}\,^1A')$ [a]		$DSS^-(\tilde{X}\,^1A')$ [b]	
(v_1,v_2,v_3)	Energy/cm^{-1}	(v_1,v_2,v_3)	Energy/cm^{-1}
(0,0,0)	0.0 [c]	(0,0,0)	0.0 [c]
(0,0,1)	478.8	(0,0,1)	478.9
(0,1,0)	808.8	(0,1,0)	588.9
(0,0,2)	953.0	(0,0,2)	953.4
(0,1,1)	1282.6	(0,1,1)	1064.0
(0,0,3)	1422.8	(0,2,0)	1172.0
(0,2,0)	1605.9	(0,0,3)	1423.4*
(0,1,2)	1751.8	(0,1,2)	1534.7*
(0,0,4)	1888.4	(0,2,1)	1643.1*
(0,2,1)	2074.5	(0,3,0)	1748.8*
(0,1,3)	2216.6*	(1,0,0)	1791.6
(0,0,5)	2350.5	(0,0,4)	1889.2*
(0,3,0)	2390.6	(0,1,3)	2000.9*
(1,0,0)	2453.6	(0,2,2)	2109.8*
(0,2,2)	2538.5*	(0,3,1)	2215.8*
(0,1,4)	2677.6*	(1,0,1)	2272.6*
(0,0,6)	2808.0*	(0,4,0)	2319.3
(0,3,1)	2853.9*	(0,0,5)	2351.1
(1,0,1)	2938.1	(1,1,0)	2374.2*
(0,2,3)	2998.2*	(0,1,4)	2463.5
(0,1,5)	3139.9*	(0,2,3)	2572.2*
(0,4,0)	3162.8	(0,3,2)	2678.5
(1,1,0)	3250.5	(1,0,2)	2750.4*
(0,0,7)	3264.5*	(0,1,4)	2782.3*
(0,3,2)	3312.6*	(0,0,6)	2809.2*
(1,0,2)	3414.9	(1,1,1)	2851.9
(0,2,4)	3455.5*	(0,5,0)	2883.6*
(0,1,6)	3593.7*	(0,1,5)	2925.5*
(0,4,1)	3620.9*	(1,2,0)	2951.3*
(0,0,8)	3732.7*	(0,2,4)	3031.9

a) Zero point vibrational energy (G_0) = 1926.1 cm^{-1}. c) Reference energy.

b) Zero point vibrational energy (G_0) = 1459.4 cm^{-1}.

Figure Captions:

Figure I: MRCI+Q one-dimensional cuts of the PESs of the electronic states of HSS^- (thin lines) together with those of HSS($\widetilde{X}\,^2$A" and 1^2A') (thick lines) for bent structures. These curves are given along the SS (R_{SS}, in A) and SH (R_{SH}, in B) internal coordinates. The remaining coordinates are kept fixed at R_{SH} = 2.5 bohr or R_{SS} = 3.9 bohr and θ = 102° corresponding to their equilibrium values in HSS^- ($\widetilde{X}\,^1$A'). These curves are given in energy with respect to the HSS (X^2A") minimum.

Figure II: MRCI+Q one-dimensional cuts of the PESs of the electronic states of HSS^- (thin lines) together with those of HSS ($\widetilde{X}\,^2$A" and 1^2A') (thick lines) along the bending coordinate. The SH and SS distances are set to 2.5 and 3.9 bohr, respectively. These curves are given in energy with respect to the HSS ($\widetilde{X}\,^2$A") minimum.

Figure III: Collinear MRCI+Q one-dimensional cuts of the PESs of the electronic states of HSS^- (thin lines) together with those of HSS($\widetilde{X}\,^2\Pi$ and $^4\Sigma^-$) (thick lines) along the SS (R_{SS}, in A) and SH (R_{SH}, in B) stretches. The remaining coordinates are kept fixed at their equilibrium values in HSS^- ($\widetilde{X}\,^1$A'). These curves are given in energy with respect to the HSS ($\widetilde{X}\,^2$A") minimum.

Figure I A

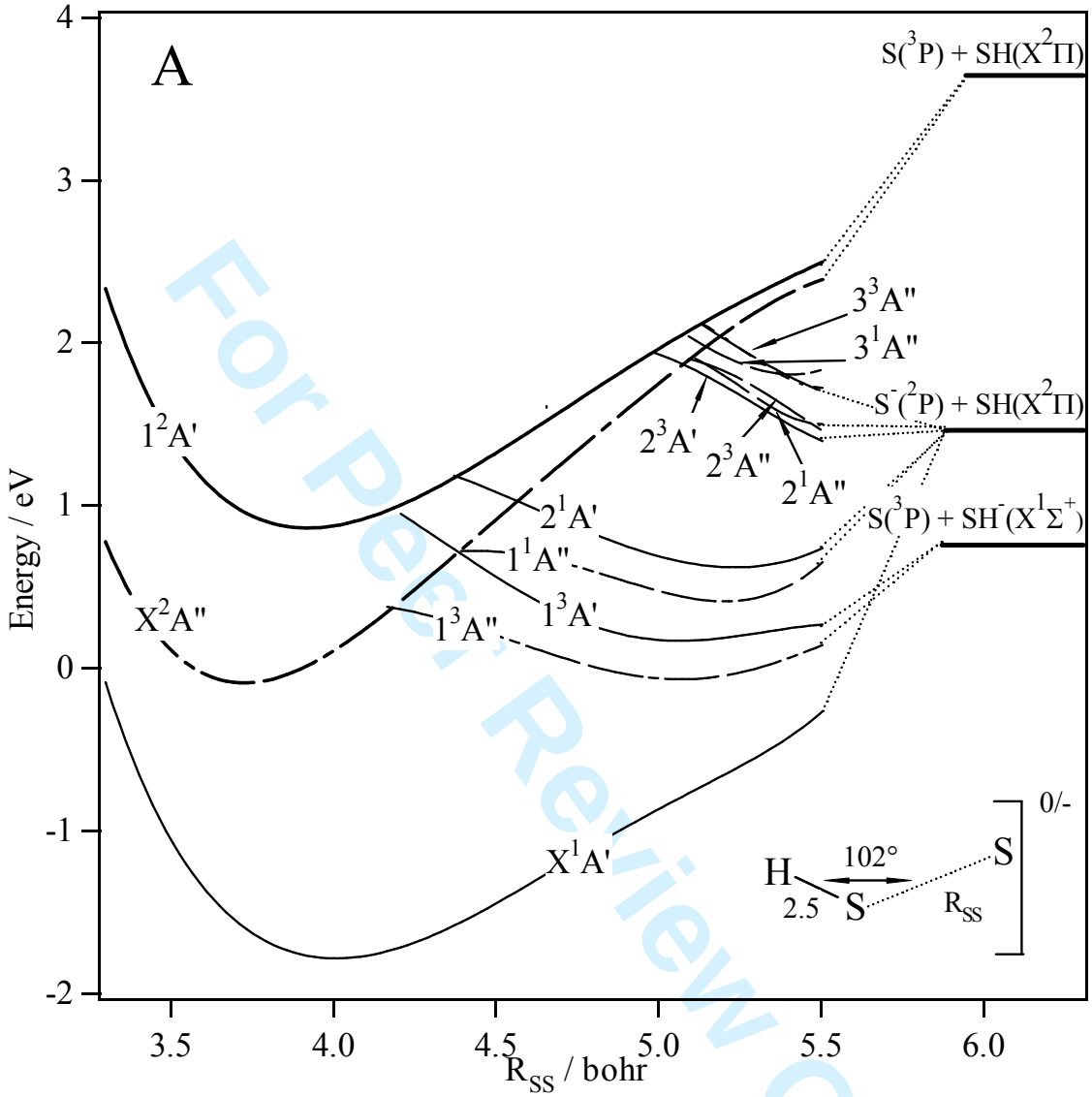

Figure I B

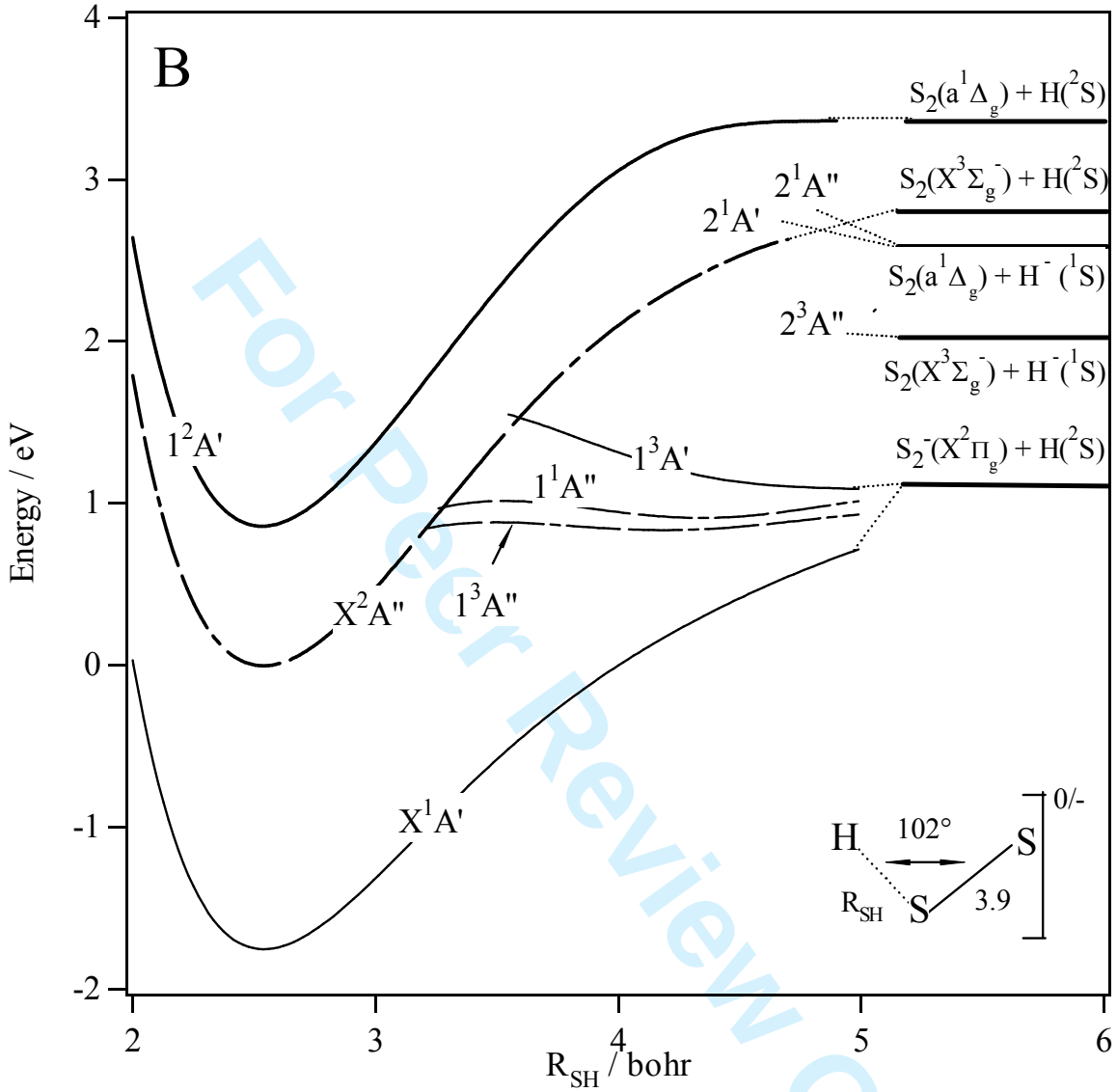

Figure II

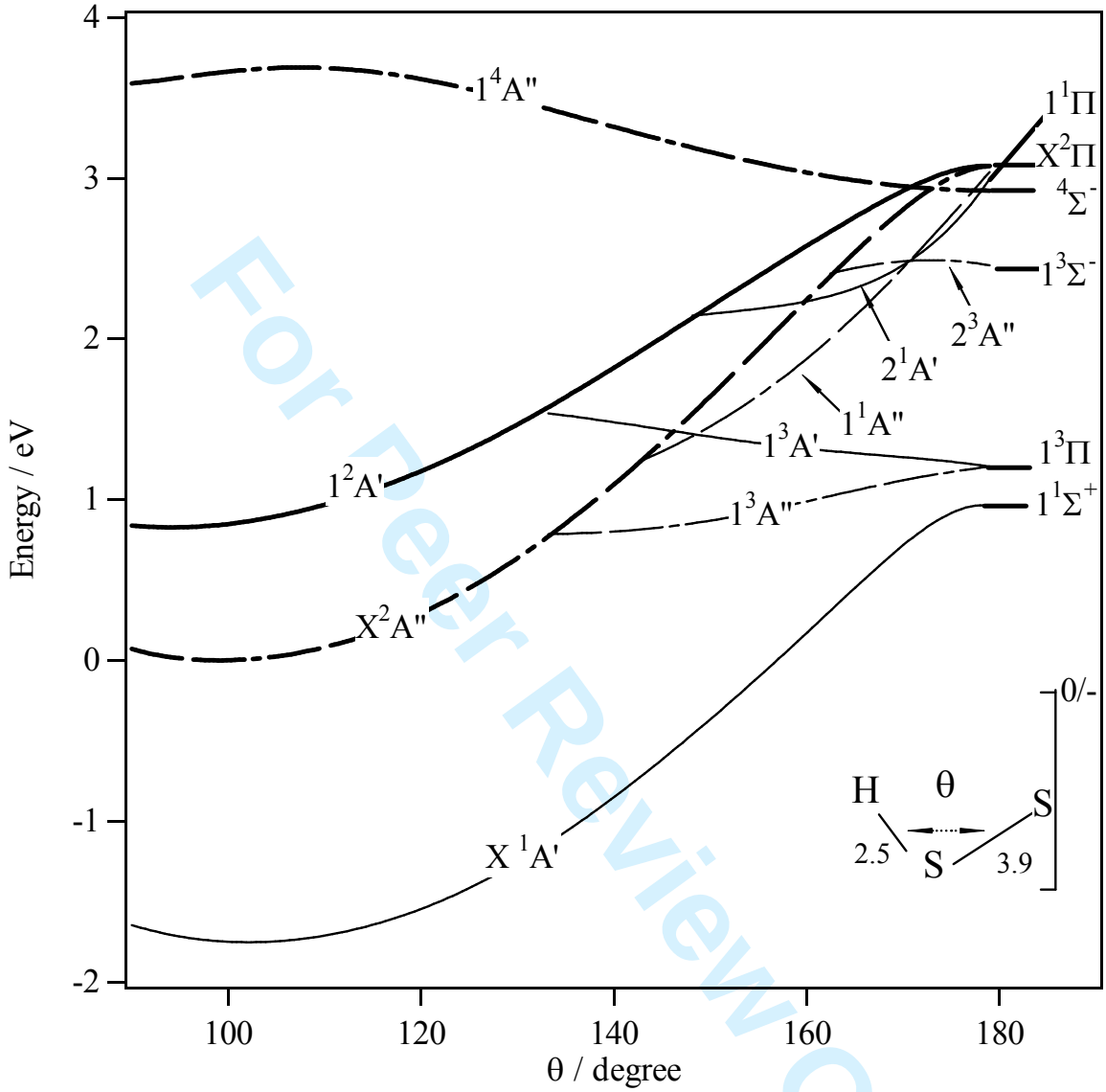

Figure III A

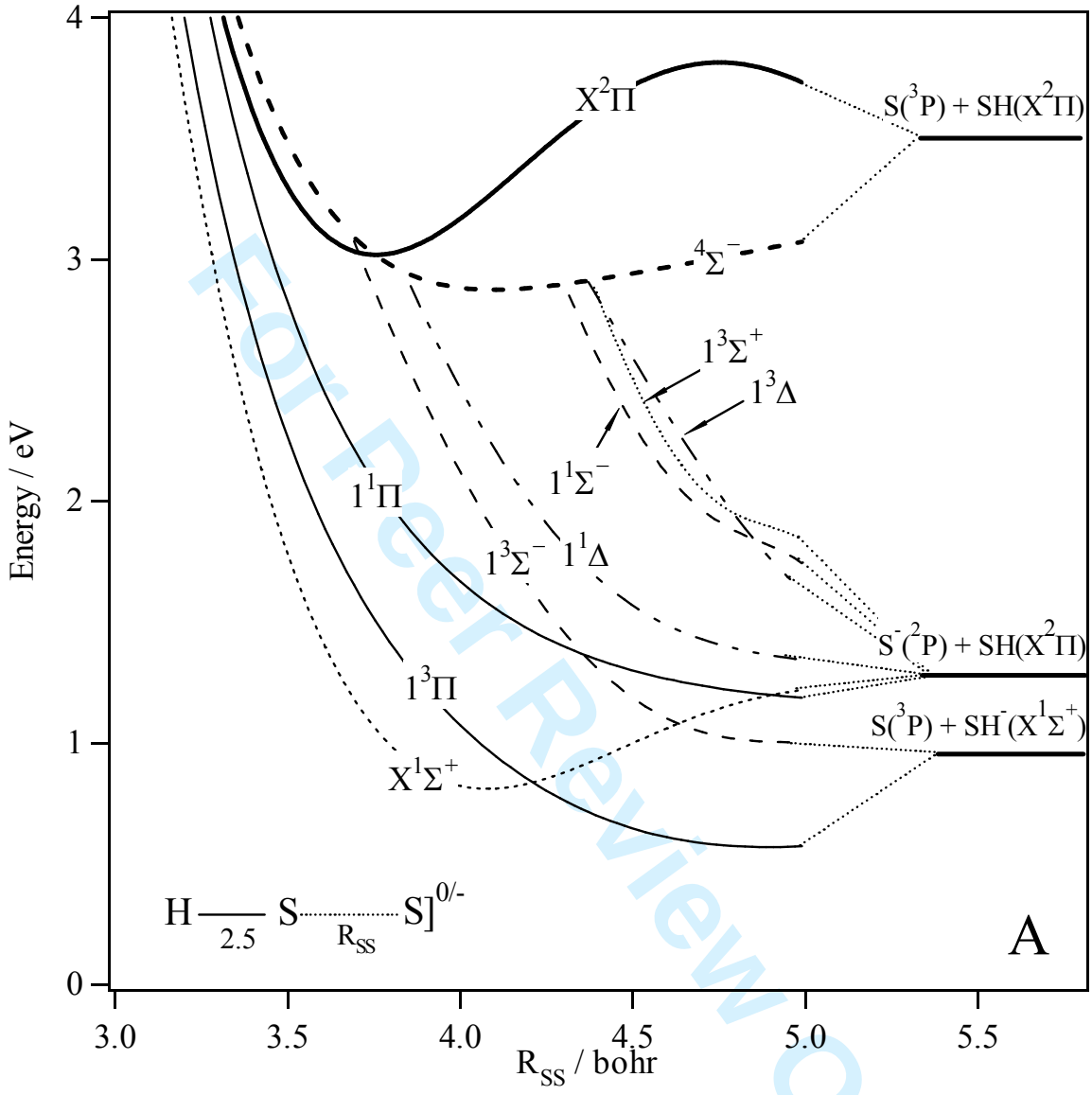

Figure III B